Published in: Applied Surface Science 161 (2000) 497-507

Interaction of potassium with Fe_3O_4(111) at elevated temperatures.

Sh. K. Shaikhutdinov* , W.Weiss, R.Schlögl

Department of Inorganic Chemistry, Fritz-Haber-Institute of the MPG, Faradayweg 4-6, 14195 Berlin, Germany

* Corresponding author: e-mail, shaikhutdinov@fhi-berlin.mpg.de, m phone +49 30 8413 4190

Submitted 23 March 2000; accepted 28 April 2000

Abstract

The surface structures formed by annealing of the potassium overlayer on the Fe_3O_4(111) surface were investigated by low electron energy diffraction (LEED), Auger electron spectroscopy (AES) and scanning tunneling microscopy (STM). Annealing at 600-700°C in vacuum or 10^{-6} mbar of oxygen resulted in well-ordered surfaces depending on the amount of potassium pre-deposited. As the K coverage increased, it transformed gradually from a (4x4) to a (2x2) and then to a (1x1) structure relative to the original Fe_3O_4(111)-(1x1) surface. At low coverage, the (4x4) structure was formed by a long-range modulation of the surface with an ~24 Å periodicity which exhibited an internal 6 Å periodicity characteristic for the Fe_3O_4(111)-(1x1) surface. At mid-coverage, two sorts of (2x2) domains were observed, which were distinguished by the different diameter of protrusions forming a STM image. They were attributed to the different states of potassium in top layer. These domains coexisted on the surface and were found at both oxidative and vacuum preparations. At high K coverage, the surface exhibited a (1x1) structure with a high density of vacancy defects. Auger depth-profile measurements confirmed the diffusion of potassium into iron oxide bulk at elevated temperatures. The formation of a non-stoichiometric $K_2O/K_2Fe_{22}O_{34}/Fe_3O_4$(111) interface with a gradual decreasing of potassium concentration from the surface has been suggested.

Key words:
Alkali metals, iron oxide, potassium, potassium iron oxide, scanning tunneling microscopy, surface reconstruction.

PACS: 68.35.B; 68.35.Bs, 81.65.M; 71.20.D

1. Introduction.

The promoting effects of the alkali metals (AM) are well established in catalysis [1, 2]. Current progress in understanding AM's adsorption on metal surfaces has been recently reviewed by Diehl and MacGrath [3], which revealed debates so far existing in this field. Less is known about AM interaction with oxide surfaces since experimental data are relatively scarce (see review of Campbell [4]). Most of the data relates to the adsorption on the single crystal TiO_2(110) and NiO surfaces (e.g., refs. 5-7 and references therein), and only a few of these studies have been reported on the interaction of alkali metals with other oxide surfaces like for example MgO(100) [8], Cr_2O_3(0001) [9], FeO(111)/Pt(111) [10] and quite recently on Na adsorption on the Fe_3O_4(111)-terminated α-Fe_2O_3(0001) surface [11].

At submonolayer coverage, alkali ad-atoms occupy specific sites offered by the oxide lattice, which is frequently a hollow-like site formed by oxygen anions so that AM atoms can maximize their coordination with the oxygen layer [4]. As coverage increases, an alkali metal overlayer grows predominantly by the Stranski-Krastanov mode via formation of three-dimensional islands on the first layer wetting an oxide surface [4]. Oxidation of thick AM overlayers at room temperature produced various AM oxides, their states were found to depend on a metal coverage, oxygen pressure and exposure [8,12].

Recently, we have investigated the structure and adsorptive properties of the different iron oxide surfaces, FeO (111), Fe_3O_4 (111) and α-Fe_2O_3 (0001), prepared by the epitaxial growth onto a Pt(111) substrate [13-18]. The oxide films were used as model catalysts for the dehydrogenation of ethylbenzene to styrene. This important industrial process is performed on potassium promoted iron oxide catalysts in the presence of steam at ~600°C. Potassium was found to increase the catalytic activity by about an order of magnitude [19]. For the catalysts preparation, the appropriate amounts of Fe_2O_3 and K_2CO_3 (~10-30 wt.%) were calcined in air at ~600°C. Mühler et al.

[20,21] have suggested that the active catalyst phase under reaction conditions corresponds to a thin $KFeO_2$ film supported on a solid solution of $K_2Fe_{22}O_{34}$ in Fe_3O_4. The $K_2Fe_{22}O_{34}$ phase acts as a storage medium from which the surface is continuously supplied with a near monolayer coverage of potassium ions. This potassium migration causes a continious solid-state transformation of the catalyst during its lifetime.

In order to investigate the surface structures of potassium promoted iron oxides and a structural effect of potassium on a catalytic activity, first we need to prepare a well defined potassium iron oxide surface for which there are no adopted rules so far. Secondly, it is important to study the surface structures formed at reaction temperatures, that is about 600°C in the above mentioned reaction. Therefore, in the present work, we use a deposition of metallic potassium onto the $Fe_3O_4(111)$ surface followed by annealing at elevated temperatures. We varied the amount of potassium deposited, annealing temperature and ambient conditions (oxygen, vacuum). The criterion was the observation of any ordered structure monitored by low energy electron diffraction (LEED). The resulting structures were investigated by scanning tunneling microscopy (STM) and Auger electron spectroscopy (AES) at room temperature.

2. Experimental.

The experiments were performed in an ultra-high vacuum chamber (a base pressure below $1x10^{-10}$ mbar) equipped with AES, LEED, STM and other surface science facilities [22]. Preparation of the $Fe_3O_4(111)$ epitaxial films has been described in detail elsewhere [13, 18]. Briefly, metallic iron was evaporated onto a clean Pt(111) substrate and then oxidized in 10^{-6} mbar O_2 at ~700°C. By many deposition-oxidation cycles, an $Fe_3O_4(111)$ film up to ~500 Å thick can be prepared.

Potassium was evaporated onto clean $Fe_3O_4(111)$ substrate kept at room temperature, using a commercial (SAES) getter source. The pressure did not exceed $2x10^{-9}$ mbar during K deposition. The sample was placed about 1.5 cm from the K source. The K coverage, measured by AES, was uniform throughout the sample. Subsequently, the $K/Fe_3O_4(111)$ samples were annealed at 600-700°C in 10^{-6} mbar O_2 or in vacuum. In some preparations, we used repeated deposition-annealing (or deposition-oxidation) cycles in order to get a high K coverage.

AES measurements were performed with a 3kV primary beam and a modulation amplitude of ~10 V. STM images presented here were obtained at bias voltage of about 1.4 V applied to the sample and at tunneling current ca. 1 nA. In general, no significant changes were found by switching a bias polarity.

3. Results.

The Fig. 1 displays side (a) and top (b) views of the $Fe_3O_4(111)$ surface. Previous dynamical LEED and STM studies combined with ab-initio calculations have proved that this surface is terminated by a ¼ ML of the Fe^{3+} ions in 3-fold hollow sites over the close-packed oxygen layer defined as 1ML [14]. This creates a hexagonal (1x1) unit cell indicated in Fig. 1b with a 5.94 Å lattice constant. The outermost Fe cations produce a hexagonal lattice of protrusions with a ~6 Å periodicity in high resolution STM images presented elsewhere [13, 14, 18].

3.1. AES and LEED study of K/Fe_3O_4 surface.

Fig. 2a shows a typical AES spectrum of the $K/Fe_3O_4(111)$ surface. Annealing of the K overlayer at elevated temperatures results in a strong decrease of the K (252 eV) Auger signal. This can be explained by the fact that the metallic potassium is thermally desorbed at ~250°C [18]. However, a significant part of the K atoms can diffuse into the bulk. This is confirmed by the Auger depth-profile measurements, as presented in Fig. 2b, showing temporal evolution of the K(252 eV), O(510 eV) and Fe(652 eV) peak intensity while the annealed at 700°C surface is exposed to 500 eV Ar+ -ions at a current density of ~2 $\mu A/cm^2$. Under the conditions used, 5 min of ion bombardment approximately corresponds to removing of few monolayers. Excluding a preferential sputtering effect, if any, the results show that potassium can penetrate into the oxide bulk ~10 monolayer in depth depending on the sample pre-history: the more K pre-deposited, the deeper it was found. Annealing of the sputtered sample at 700°C in vacuum or in 10^{-6} mbar of oxygen resulted in a surface segregation of potassium as indicated by arrows *a* and *b* in Fig. 2c.

Therefore, we cannot determine the amount of K in top layer precisely, since AES averages the chemical composition of the surface as thick as the Auger electron escape length, i.e., 10-20 Å. On other hand, this allows us to estimate a chemical composition of the surface region using a general formalism of quantitative AES analysis for homogeneous compounds. Given the Auger sensitivity factor of 0.75, 0.5 and 0.2 for K(252 eV), O(510 eV) and Fe(652 eV) peaks, respectively [22], the surface composition can be formally written as KFe_xO_y where x~1.1-0.9 and y~1.3-2.0 depending on K coverage. We will use the standard term "coverage" just to indicate the overall amount of K within surface region. To characterize the K coverage semi-quantitatively we have used K to O peak intensity ratio ($I_K : I_O$). Therefore, "low", "mid-" and "high" coverage corresponds to $I_K : I_O$ <0.5, ~0.7 and ~1.0, respectively.

Fig. 3 shows the characteristic LEED patterns of the samples all treated in 10^{-6} mbar O_2 at 700°C but possessing different amounts of K. When compared with the pattern of the original $Fe_3O_4(111)$ surface shown in Fig. 3(a), the LEED patterns from the K-doped surfaces exhibit additional diffraction spots and a remarkably increased background intensity. At low K coverage, these spots appear as

satellites around the spots coming from the original Fe_3O_4(111)-(1x1) structure (Fig. 3b). This pattern can be described as a commensurate (4x4) superstructure relative to Fe_3O_4(111)-(1x1) as indicated by the corresponding unit cells. At K mid-coverage, a commensurate (2x2) structure is clearly seen in Fig. 3c. As the K coverage increases, the (2x2) structure vanishes, and LEED pattern exhibits only the diffused spots of a (1x1) structure as shown in Fig. 3d. Thus, the surface undergoes a (4x4)→(2x2)→(1x1) structural transformation as the K coverage increases.

Combined AES and LEED data obtained on the different samples prepared by annealing in oxygen and in vacuum are summarized in Table. The Table also contains the values of I_{Fe} : I_O ratio in order to monitor a stoichiometry of the Fe_3O_4(111) phase as a host material. For both preparations, the results show that the I_{Fe} : I_O ratio decreases as the I_K : I_O ratio increases. This correlation is also observed during the ion sputtering experiments as shown in Fig. 2c, where the I_{Fe}:I_O ratio increases as potassium is removed by sputtering.

3.2. STM study of K/Fe_3O_4 surface.

STM images of the original Fe_3O_4(111) surfaces (not presented here for conciseness) revealed the atomically flat ~1,000 Å wide terraces separated by monoatomic steps of ~5 Å in height. High resolution STM images exhibited a hexagonal lattice of protrusions with a 6 Å periodicity assigned to the outermost iron cations [14].

The large-scale STM image presented in Fig. 4a shows that the mesoscopic roughness of the potassium doped iron oxide surface at low K coverage is not changed after oxidation at 700°C. Again, smooth large terraces separated by the atomic steps running along main crystallographic directions were observed. At K mid-coverage, the surface oxidized at 600°C exhibited numerous islands of ~100 Å in size, which were randomly distributed on the terraces (Fig. 4b). When this surface was further oxidized at 700°C, only large triangular terraces of 500-1,500 Å in size were observed as shown in Fig. 4c. As the K coverage increased, no remarkable changes in the large-scale morphology were found.

Close STM inspection of the surfaces at low K coverage revealed two regions labeled α and β in Fig. 5a. They were separated by steps of either 2.5 or 5 Å as measured by profile lines shown below the image (a). There were also some dislocations seen within α-regions as protruding lines, for example, in the upper-right part of Fig. 5a. Regions α exhibit a hexagonal lattice of protrusions with a ~12 Å periodicity that is twice of the lattice constant on the Fe_3O_4(111)-(1x1) surface (5.94 Å). Therefore, this surface must be assigned to the (2x2) structure detected by LEED measurements presented in Section 3.1. The (1x1) sub-lattice cannot be resolved on these regions therefore a registry between (2x2) and (1x1) lattices is not determined.

Fig. 5c shows a high resolution STM image of the β-region. The surface exhibits a long-range periodic modulation with corrugation up to ~1.5 Å, creating triangular domains in turn formed by protrusions with an ~6 Å spacing therein. The atomic structure of the individual domain is shown in the inset of this image. On a large scale, the domains are arranged on the surface in a periodic manner as a nearly close-packed structure. This is evidenced by two-dimensional fast Fourier transform (2D-FFT) of the STM images. One of the 2D-FFT maps obtained from the STM images, where both α and β regions have been resolved, is shown below Fig. 5a. Three series of six equidistant spots indicated by arrows are aligned and correspond to the hexagonal structures with an ~6, ~12 and 24(±2) Å periodicity and therefore are assigned to the (1x1), (2x2) and (4x4) surface structures, respectively.

Fig. 6a shows the high resolution STM image of the surface exhibited the numerous patches in the large-scale STM image presented in Fig. 4b. Again, domains showing a hexagonal structure with a 12 Å periodicity corresponding to the (2x2) structure are imaged. However, the surface region shown with a higher contrast in the left-bottom corner of the image also manifests the (2x2) symmetry, but the protrusions forming it are significantly narrower. This is better resolved in Fig. 6b where two sorts of (2x2) domains neighbor on the same height level. The dislocation splitting the surface to few domains is clearly seen in this image as indicated by the broken lines. The half-widths of the protrusions are measured to be of ~6 Å and ~4 Å for the surfaces termed "ball"- and "dot"-surfaces, respectively. The fact that the "ball"-surface is normally clean while the "dot"-surface looks like covered by adsorbates also indicates their distinct chemistry. The profile line measured over single domain and shown below the image reveals that both sorts of protrusions are in registry, which means that they occupy the same sites.

Another structure which is resolved in the right-hand part of Fig. 6a is the corrugated surface, which exhibits an internal ~6 Å periodicity. This structure resembles the α-regions shown in Fig. 5c, which we assigned to the (4x4) structure. It seems plausible that these domains, which have been detected after oxidation at lower temperature (600°C for 2 min) and have disappeared after further treatment at 700°C for 5 min, correspond to the surface not being completely transformed to the (2x2) structure.

At high K coverage, STM images revealed fewer domains with the (2x2) structure. Now, most of the surface exhibits a hexagonal (1x1) structure with an ~6 Å periodicity, however, it is characterized by a high density of vacancy defects (Fig. 7a). This observation is in line with the LEED pattern shown in Fig. 3d where the "(2x2)" spots vanish and the "(1x1)" spots get diffused due to the highly defective surface. STM images in Fig. 7b,c display an interface between the (1x1) and (2x2) domains, which show that the "(2x2)"-dot protrusions are in registry with those forming the (1x1) lattice. This means that all the protrusions on these images occupy the same sites.

The surfaces prepared by vacuum annealing exhibit, in principle, the similar structures as those observed by preparation in oxidative conditions (see Table). Two STM images in Fig. 8 demonstrate this: the image (a) presented with the differentiated contrast shows the

(2x2) "ball"- and "dot"-surfaces separated by step of ~2.5 Å; the image (b) shows the highly defective (1x1) surface formed at high K coverage.

4. Discussion.

We start the preparation of the K-doped iron oxide surface with a deposition of metallic potassium at room temperature. In order to observe detectable changes in the surface structures of annealed samples, we deposited about 5 ML of potassium, as estimated from AES spectra. The corresponding LEED patterns showed very weak and diffused diffraction spots, if any, coming from the Fe_3O_4(111)-(1x1) substrate. Therefore, both AES and LEED results indicate a thickness of a K overlayer no more than a few monolayers.

Annealing of the K-covered iron oxide surface at 600-700°C strongly decreases the amount of potassium on the surface. This is in part due to K ad-atoms desorbing at ~250°C [18], however, a significant part of the K atoms reacts with the oxide. Auger depth-profile measurements presented in Fig. 2 show that the potassium concentration gradually decreases along the distance from the surface and can be detected at ~10 monolayer deep.

Interaction of potassium and iron oxide forms a non-stoichiometric surface phase, which could be formally written as KFe_xO_y, where *x* and *y* vary between 0.5-1 and 1-2, respectively. A search in the structural database [24] resulted in several ternary potassium iron oxide compounds, which show comparable amounts of K and Fe. They are $KFeO_2$ (an ortorhombic space group P*bca*, lattice parameters *a*=5.60, *b*=11.25 and *c*=15.90 Å), K_3FeO_2 (a tetragonal space group P 4_1 2_1 2, *a* = *b* = 6.05, *c*=14.03 Å) K_3FeO_4 (an ortorhombic space group P*nma*, *a*=7.70, *b*=9.09 and *c*=7.84 Å), $K_6Fe_2O_6$ (a monoclinic space group C *1 2/m 1*, *a*=7.13, *b*=11.12 and *c*=6.51 Å) and K_3FeO_4 (an ortorhombic space group P*nma*, *a*=7.70, *b*=5.86 and *c*=10.34 Å). Note, that Fe_3O_4 has a space group F*d3/m* and lattice parameters *a* = *b* = *c* = 8.4Å.

We could not find any plane in the above listed compounds which would exhibit a hexagonal symmetry and fit the hexagonal Fe_3O_4(111) substrate surface. In addition, a formation of such a compound on the surface must drastically change a LEED pattern. In contrast, Fig. 3 shows no visible changes of the (1x1) lattice parameter at any K coverage studied (more precise SPA-LEED measurements could prove this). It should be also mentioned that, for example, the $KFeO_2$ compound is normally prepared by calcination of Fe_2O_3 and K_2CO_3 at ~1000°C in air. A thin $KFeO_2$ film was observed by Muhler et al. on the technical K-promoted iron oxide catalysts only under reaction conditions of dehydrogenation of ethylbenzene to styrene in the presence of steam at 600°C and at atmospheric pressure [21]. Both preparation conditions are much more severe than those used in this present work. Therefore, we can rule out the formation of $KFeO_2$ and other mentioned phases as being responsible for the surface structures found.

Meanwhile, AES results show that the $I_{Fe} : I_O$ ratio decreases as the $I_K : I_O$ ratio increase (see Table and Fig. 2c). In other words, the more potassium the less iron within surface region. This fact together with the conservation of the surface symmetry during solid state reaction could be explained by assuming that potassium substitutes part of the iron ions. It has been previously suggested, that the AM adsorption on metals can produce the formation of such a "substitutional" phase at high AM coverage (see review [3]). On the other hand, the ionic radius of potassium (1.33 Å) is much larger than of iron cation (0.78 Å) [25]. Therefore, this substitutional phase would result in a strong strain and hence a large number of dislocations and other structural defects, which were actually found in the STM images as presented in Fig. 5-7.

Another possible candidate for the surface phase produced is a $K_2Fe_{22}O_{34}$ or a $K_2O{\cdot}(Fe_2O_3)_{11}$ compound which has a hexagonal space group $P6_3/mmc$ (lattice parameters *a*=5.92 and *c*=23.79 Å.) and is formed from two spinel-like blocks with a layer of potassium oxide inbetween [26]. The potassium layer is not dense, giving rise to a non-stoichiometry of K:Fe between 1:11 and 1:5 [20]. This surface phase would fit the hexagonal Fe_3O_4(111) substrate well, since it has a lattice constant identical to the original Fe_3O_4(111) surface (5.94 Å) and would maintain the surface unit cell as judged by LEED. However, the potassium to iron ratio in the latter compound is much lower than that measured by AES on the surfaces prepared, i.e., about 1:1, assuming a homogeneous potassium distribution in near surface region. This indicates that the top layers are enriched with potassium and can be attributed, for example, to the surface terminating with potassium oxide. The latter seems quite reasonable during oxidation of K overlayer in 10^{-6} mbar of O_2. Indeed, it has been found that interaction of oxygen with K multilayers on Si(111) and MgO(100) substrates results in various potassium oxide phases, depending on oxygen pressure and temperature [8,12]. However, the surface structures formed on iron oxide in this work are very similar for both oxidative and vacuum preparations. This indicates that the potassium react with lattice oxygen of iron oxide as well. A similar conclusion has been drawn by Chen et al. based on HREELS and TPD study of the K/NiO/Ni(100) surface annealed to 900K in vacuum [5]. Ion surface scattering experiments performed by Vurens et al. also revealed that potassium deposited on the FeO monolayer grown on Pt(111) after heating to 950K remains in the outermost layer [10].

Thus, we suggest that the interaction of potassium with Fe_3O_4(111) at elevated temperature leads to the formation of a non-stoichiometric $K_2O/K_2Fe_{22}O_{34}/Fe_3O_4$ interface with a gradual decreasing of the K content from the surface into the oxide bulk. The surface structures formed depend on the K coverage.

At low K coverage, the LEED pattern in Fig. 3b and the STM image in Fig. 5c show the (4x4) superstructure which is created by a long-range modulation of the surface in turn formed by protrusions with a 6 Å periodicity, which is characteristic for the Fe_3O_4(111)-(1x1) surface. The inset in Fig. 5c shows that the adsorbed on top site atom seems to modify the electronic structure of the neighboring atoms, resulting in apparent modulation of the Fe_3O_4(111) surface. Another possibility that this modulation is caused by the K-induced surface de-relaxation of the original Fe_3O_4(111) surface which is strongly relaxed under vacuum conditions [27].

It is interesting to note, that if we put a side not perfect ordering the STM images of the (4x4) structure look similar to those obtained on layered compounds, which exhibit a charge density waves (CDW) phenomenon, for example, on 1T-TaS_2 [28]. The CDW structure is formed by so called "Star-of-David" clusters including thirteen Ta atoms and manifest itself in the STM images as a hexagonal long-range modulation with an ~12 Å periodicity of the surface formed by a hexagonal lattice with an internal ~3 Å periodicity. This similarity can suggest some interesting analogies since the charge transfer from potassium to oxide obviously occurs due to the lower ionization potential of potassium, which redistribute the ratio of Fe^{3+} and Fe^{2+} states within a surface region as found by XPS [11].

At K mid-coverage, the (2x2) structure covers almost the entire surface. However, we observe two different (2x2) structures which are formed by the protrusions with different width, ca. 6 and 4 Å, respectively (Fig. 6). Previous STM studies of the AM adsorption on oxide surfaces show that the alkali metal atoms are imaged as protrusions [6,29]. (With the metal substrates, the STM results are somewhat confused since, for example, potassium on Cu(110) has been imaged as depression or protrusion depending on the tip conditions and the tunneling parameters [30].) However, the alkali metals were found always to form the outermost layer even after heating to elevated temperatures. Therefore, we assigned the STM protrusions to the position of the K atoms in the top layer. Our STM observation of the two different domain structures indicates the different states of potassium in the top layer or the different terminations of the non-stoichiometric potassium iron oxide phase suggested above.

As the K coverage increases, the (2x2) structure vanishes and the surface again manifests the (1x1) symmetry. This surface can definitely not be attributed to the original Fe_3O_4(111)-(1x1) surface, because there is too much potassium within the surface region. The (1x1) structure is probably produced from the (2x2) structure, as the K coverage gets saturated. The STM images in Fig. 7b,c show that both (2x2) and (1x1) protrusions are in registry, which means that they occupy the same sites. The (2x2)-"dot" protrusions are only 0.1 Å higher, this small height difference could be attributed to the different surface relaxation within (2x2) and (1x1) unit cells.

One should also keep in mind that the STM tip probes the local density of electronic states, therefore, an STM image includes not only a topographic but also an electronic factor. It means, for example, that a "guest" atom imbedded in the layer of the "host" material could be seen as a protrusion or a depression atom despite having nearly the same geometrical size. Therefore, the surface composition and structure of the top layers formed during K-Fe_3O_4(111) interaction at elevated temperatures could not be deduced from STM measurements only. Further experiments using a photoelectron spectroscopy and an ion scattering spectroscopy are in progress in order to elucidate a detailed structure of the potassium iron oxide surfaces.

Finally, our results show that the potassium iron oxide surface undergoes a consecutive (4x4), (2x2), (1x1) reconstruction as the K coverage increases. In the case of "simple" adsorption, this type of coverage dependence indicates a repulsive interaction between adsorbed species. But in the present study, the (N x N)-structures were formed after heating at elevated temperature only and not immediately after K deposition at room temperature. However, this analogy seems quite interesting.

5. Conclusions.

Well ordered potassium doped iron oxide surfaces are formed by deposition of metallic potassium on the Fe_3O_4(111) surface and subsequent annealing at 600-700°C. The results show a close similarity between the surface structures formed by heating either in 10^{-6} mbar oxygen or in an ultra-high vacuum. It appears that these structures are thermodynamically stable and independent of the ambient conditions used.

Auger depth-profile measurements confirm the diffusion of potassium into iron oxide bulk at elevated temperatures. We suggest that the interaction of potassium and Fe_3O_4(111) leads to the formation of a non-stoichiometric $K_2O/K_2Fe_{22}O_{34}/Fe_3O_4$ interface with a gradual decreasing of the potassium concentration from the surface.

The surface structures formed depend on the K coverage. It transforms gradually from a (4x4) to a (2x2) and then to a (1x1) structure relative to the Fe_3O_4(111)-(1x1) surface as the K coverage increases. The relative brightness of the diffraction spots in the LEED patterns correlates with the surface area covered by the corresponding structures resolved by STM.

The (4x4) structure is formed by long-range modulation of the surface with a ~24 Å periodicity which in turn exhibits an internal 6 Å periodicity characteristic for the Fe_3O_4(111)-(1x1) surface. Two sorts of (2x2) domains with a 12 Å periodicity are clearly distinguished in the STM images by the width of protrusions. At high K coverage, the surface exhibits a (1x1) structure with a high density of vacancy defects.

The potassium enriched surface phase suggested in the present work is very similar to that determined as a precursor for the active phase of styrene synthesis on K-promoted iron oxide catalysts. However, the results clearly indicate that an interaction of metallic potassium and iron oxide at elevated temperatures in vacuum or low oxygen pressure does not form $KFeO_2$ compound, which are formed only during catalytic reaction.

Acknowledgement. Authors thank Dr.W.Ranke for helpful discussions.

References.

[1] Physics and Chemistry of Alkali Metal Adsorption, H.P.Bonzel, A.M.Bradshaw, G.Ertl Eds., Elsevier, Amsterdam, 1989.
[2] M.Kiskinova, Poisoning and promotion in catalysis based on surface science concepts and experiments, B.Delmon, J.T.Yates, Eds., Elsevier, Amsterdam, 1992.
[3] R.D.Diehl, R.Mcgrath, J.Phys.: Condens.Matter 9(1997) 951.
[4] C.T.Campbell, Surf.Sci.Reports, 27 (1997) 1.
[5] J.G.Chen, M.D.Weisel, J.H.Hardenbergh, F.M.Hoffman, C.A.Mims, and R.B.Hall, J.Vac.sci.Technol. A9 (1991) 1684.
[6] P.W.Murray, N.G.Condon, G.Thornton, Surf.Sci.Lett, 323(1995) L281.
[7] A.F.Carley, S.D.Jackson, J.N.O'Shea, M.W. Roberts, Surf. Sci. Lett., 440 (1999) L868.
[8] H.H.Huang, X.Jiang, Z.Zou, G.Q.Xu, W.L.Dai, K.N.Fan, J.F.Deng, Surf.Sci., 398(1998) 203.
[9] M.Wilde, I.Beauport, K.Al-Shamery, H.-J.Freund, Surf.Sci., 390(1997) 186.
[10] G.H.Vurens, D.R.Strongin, M. Salmeron, G.A.Somorjai, Surf.Sci.Lett., 199(1988) L387.
[11] J.Nerlov, S.V.Hoffmann, M.Shimomura, P.Moller, Surf.Sci. 401(1998) 56.
[12] B.Lamontagne, F.Semond, D.Roy, Surf.Sci., 327(1995) 371.
[13] W.Weiss and M.Ritter, Phys.Rev.B, 50(1999) 5201.
[14] Sh.K.Shaikhutdinov, M.Ritter, X.-G.Wang, H.Over, and W.Weiss, Phys.Rev.B., 60 (1999),
[15] Sh.K.Shaikhutdinov and W.Weiss, Surf.Sci.Lett., 432 (1999) L627.
[16] D.Zscherpel, W.Ranke, W.Weiss, and R.Schlögl, J.Chem.Phys. 108 (1998) 9506.
[17] W.Ranke, and W.Weiss, Surf.Sci. 4141(1998) 238.
[18] Sh.K.Shaikhutdinov, Y.Joseph, C.Kuhrs, W.Ranke, and W.Weiss, Faraday Discuss. 114(1999) 363.
[19] T.Hirano, Appl.Catal. 26(1986) 65, *ibid.* 28(1986) 119.
[20] M.Mühler, J.Schütze, M.Wesemann, T.Rayment, A.Dent, R.Schlögl, G.Ertl, J.Catal., 126 (1990) 339.
[21] M.Mühler, R.Schlögl, G.Ertl, J.Catal., 138 (1992) 413.
[22] W.Weiss, M.Ritter, D.Zscherpel, M.Swoboda, and R.Schlögl, J.Vac.Sci.Technol. A 16(1998) 21.
[23] L.E. Davis, N.C. MacDonald, P.W. Palmberg, P.E. Riach and R.E. Weber, Handbook of Auger electron spectroscopy, Physical Electronics Industries, Inc., Eden Prairie, MN, 1976.
[24] ICSD Collection Codes 200255, 73215, 65977, 2487.
[25] C.Kittel, Introduction to Solid State Physics, Wiley, New York, 1986.
[26] JCPDS Card [31 1034]
[27] W.Weiss, M.Ritter, Phys.Rev.B 60(1999) 5201.
[28] Sh.K.Shaikhutdinov, V.P.Babenko, D.I.Kochubey, Phys.Low-Dimens.Struct., 11/12 (1996) 109.
[29] S.J.Murray, D.Abrooks,F.M.Leibsle, R.D.Diehl, R.McGrath, Surf.Sci. 314(1994) 307.
[30] R.Shuster, J.V.Barth, G.Ertl, R.J.Behm, Phys.Rev.B 44 (1991) 13689.

Figures:

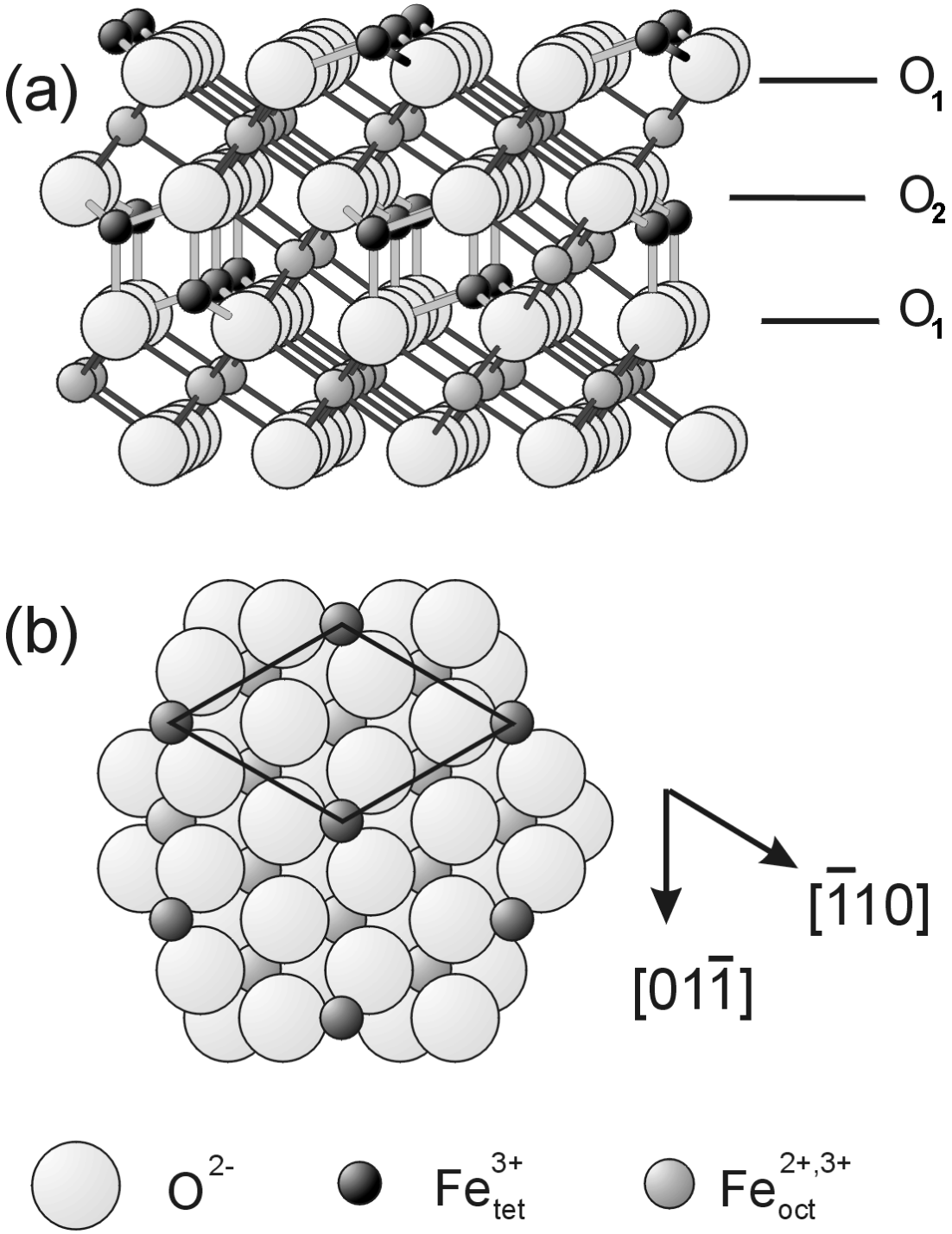

Fig. 1

Slightly tilted side (a) and top (b) views of the iron-terminated $Fe_3O_4(111)$ surface. Distance between equivalent oxygen (O_1-O_1) layers is 4.6 Å. The (1x1) unit cell with lattice constant 5.94 Å is indicated in (b).

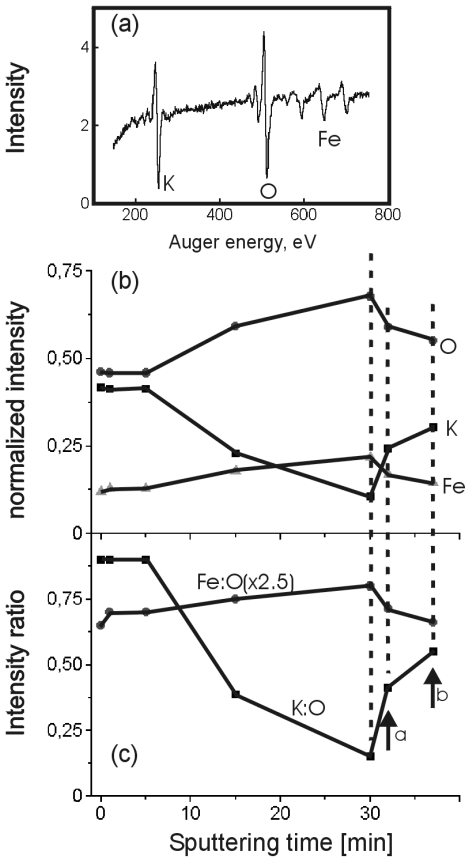

Fig. 2

(a) A typical Auger spectrum of the samples studied. (b,c) A temporal evolution of K(252 eV), O (510 eV) and Fe (652 eV) peaks intensity (b) and $I_K : I_O$ and $I_{Fe} : I_O$ intensity ratio (c) while the KFe_xO_y surface is exposed to 500 eV Ar+ ions at current density ~2 μA/cm^2. Arrows (*a*) and (*b*) indicates the resulting effect of the annealing in vacuum at 600°C for 2 min (*a*) and in 10^{-6} mbar O_2 at 700°C for 5 min (*b*).

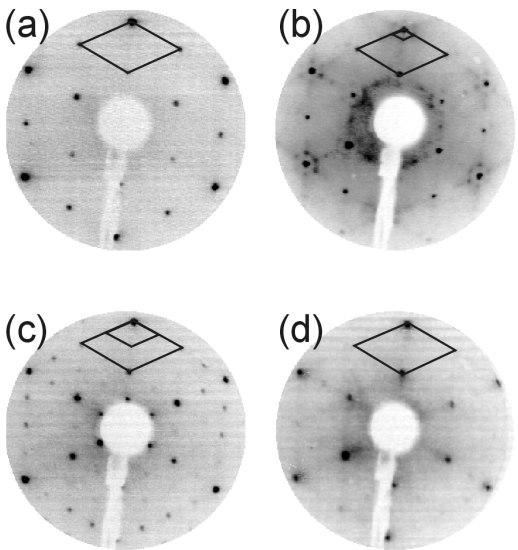

Fig. 3.

LEED patterns of the samples prepared by oxidation in 10^{-6} mbar of O_2 at 700°C possessing a different amount of potassium on the surface determined by the I_K:I_O ratio in AES spectra. (a) original Fe_3O_4(111); (b) I_K:I_O = 0.45; (c) I_K:I_O =0.7; (d) I_K:I_O =1.0. All the patterns were obtained at electron energy E=60 eV except pattern (b) which was taken at E=87 eV in order to better represent the (4x4) superstructure. The corresponding units cells are indicated.

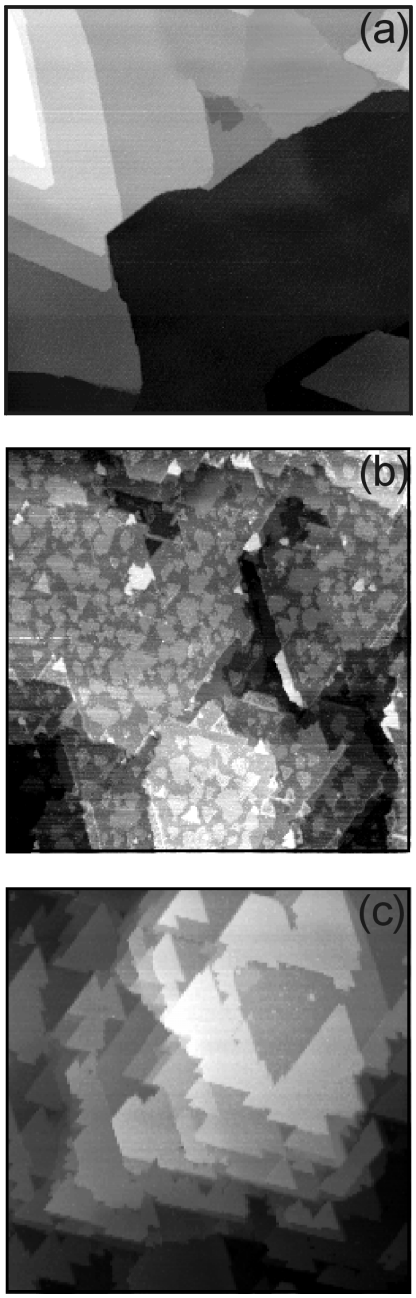

Fig. 4. Large-scale 5,000 x 5,000 Å^2 STM images of the KFe_xO_y surfaces. (a) oxidation temperature T_{ox} = 700°C, I_K:I_O = 0.45; (b) T_{ox} = 600°C, I_K:I_O = 0.7; (c) the same sample as (b) after further oxidation at 700°C. In (a) and (c), the terraces are separated by monoatomic steps of ~5 Å high running along the main crystallographic directions. Numerous islands develop on terraces by oxidation at 600°C as seen in image (b), which disappear after subsequent oxidation at 700°C (c).

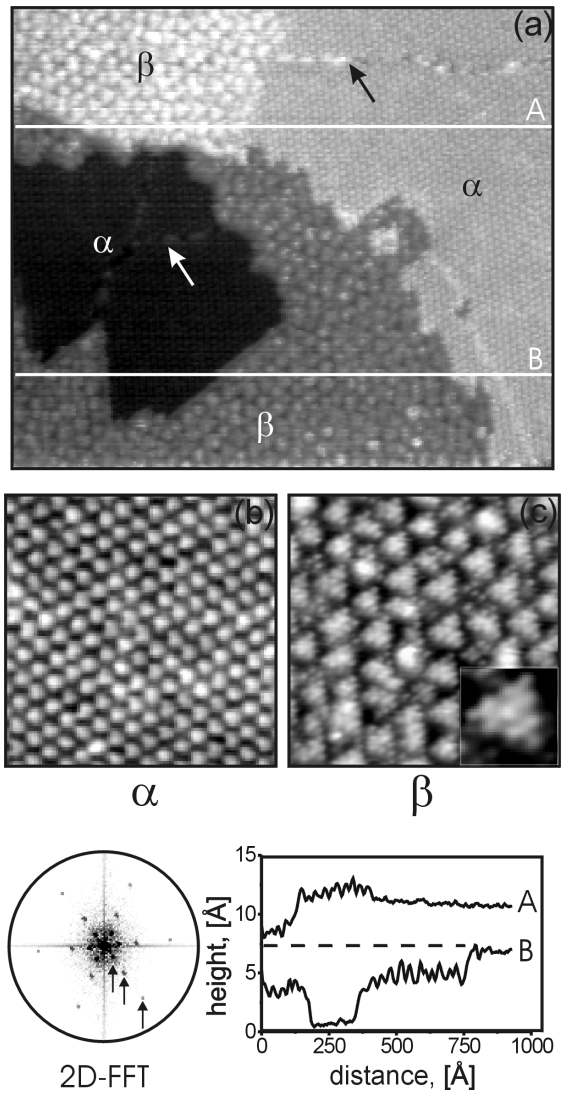

Fig. 5. 1,000 x 1,000 Å^2 (a) and 160 x 160 Å^2 (b,c) STM images of the KFe_xO_y surface at low K coverage (I_K:I_O = 0.45). Two different regions labeled α and β are clearly seen. They can be separated by steps of either 2.5 or 5 Å high as measured by profile lines shown below the image. Region α resolved in image (b) exhibits a hexagonal lattice of protrusions with a ~12 Å periodicity assigned to the (2x2) structure. Region β resolved in image (c) is characterized by a close-packed structure of triangular domains which is in turn formed by the protrusions with a 6 Å periodicity as shown in the inset. Two-dimensional fast Fourier transform (2D-FFT) obtained from the STM image (a) is shown below. Three series of six equidistant "diffraction" spots indicated by arrows are aligned and correspond to a 6, 12 and 24(±2) Å periodicity on the surface. The surface dislocations developed on both regions are indicated by the arrows.

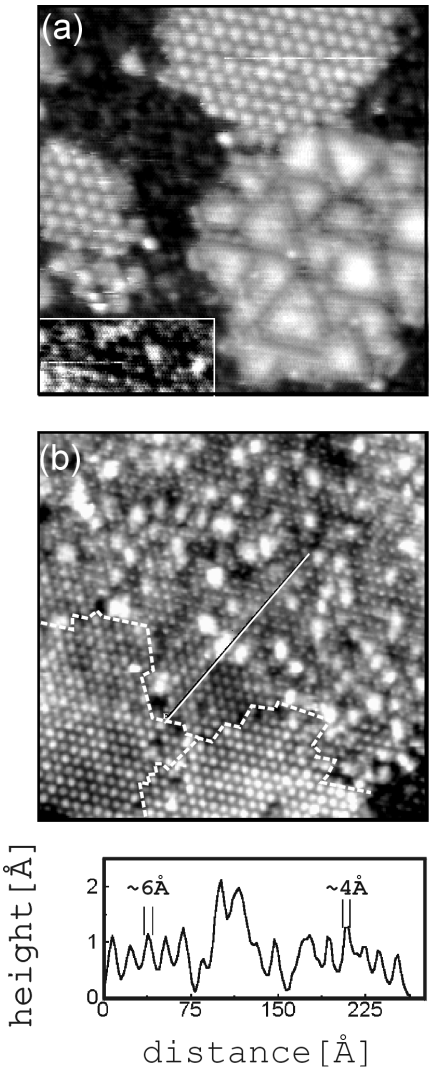

Fig. 6.230 x 230 Å^2 (a) and 490 x 490 Å^2 (b) STM images of the KFe_xO_y surface at K mid-coverage (I_K:I_O ~0.7). Image (a) shows the fine structure of the islands observed in the large-scale STM image in Fig. 4b. Two (2x2) domains with a 12 Å periodicity are visible in the upper and left-hand parts of the image (a). Left-bottom corner of the image (a) is shown with a higher contrast in order to resolve the (2x2) symmetry of this region, but having much narrower protrusions. The half-widths of the protrusions are of ~6 Å and ~4 Å. A few different (2x2) domains neighbor on the same height in the image (b). The surface dislocations are indicated by the broken line. The profile line shown below reveals both types of protrusions to be in lateral registry.

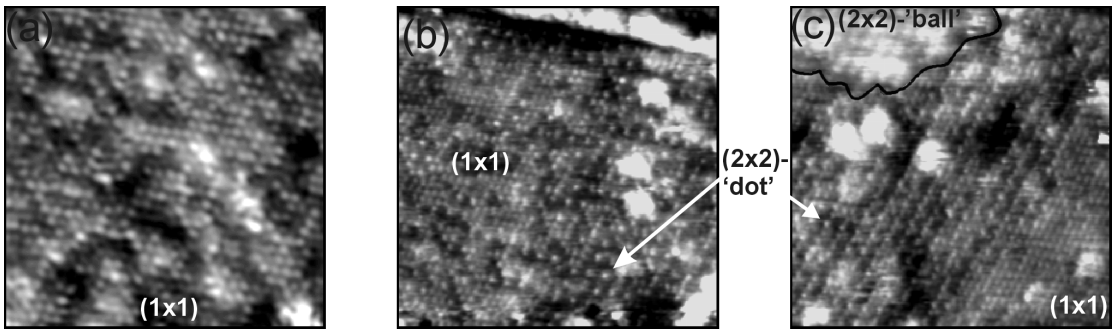

Fig. 7.

165 x 165 Å^2 (a) and 220 x 220 Å^2 (b,c) STM images of the KFe_xO_y surface at high K coverage (I_K:I_O =1.0). The surface mostly exhibits a (1x1) structure with a high density of vacancy defects as shown in (a). Images (b) and (c) show an interface between (1x1) and (2x2) "dot"-structures indicated.

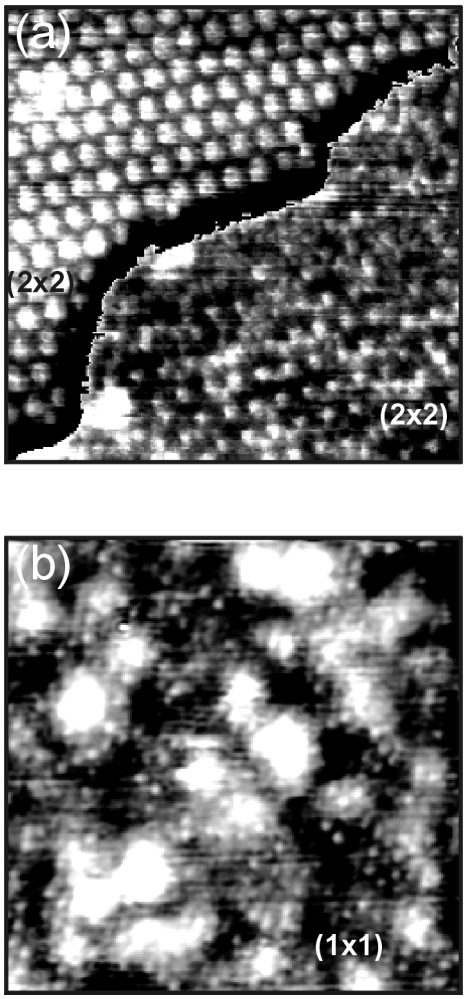

Fig. 8.

210 x 210 Å^2 (a) and 100 x 100 Å^2 (b) STM images of the potassium iron oxide surface prepared by annealing in vacuum at 700°C and corresponding to Auger ratio I_K:I_O =0.7 (a) and I_K:I_O =1.0 (b). Again, two (2x2) surfaces having the different width of protrusions are separated by 2.5 Å step in image (a). At high coverage, the (2x2) structure vanishes and the surface exhibits a highly defective (1x1) structure resolved in image (b).

Table. AES and LEED data obtained on the $K/Fe_3O_4(111)$ samples annealed at 700°C in 10^{-6} mbar of oxygen and in vacuum.

Oxygen, 10^{-6} mbar			Vacuum, $5x10^{-10}$ mbar		
AES		LEED	AES		LEED
$I_K : I_O$ (± 0.03)	$I_{Fe} : I_O$ (± 0.02)		$I_K : I_O$ (± 0.03)	$I_{Fe} : I_O$ (± 0.02)	
0	0.32	(1x1)	0.45	0.28	(1x1)
0.45	0.27	$(1x1)+(2x2)_w+(4x4)$	0.5	0.26	$(1x1)+(2x2)_w$
0.7	0.27	$(1x1)+(2x2)_s$	0.7	0.25	$(1x1)+(2x2)_s$
0.95	0.26	$(1x1)+(2x2)_w$	1.0	0.26	$(1x1)+(2x2)_w$

w- weak, *s* –strong